

This article was downloaded by:

On: 23 January 2011

Access details: *Access Details: Free Access*

Publisher *Taylor & Francis*

Informa Ltd Registered in England and Wales Registered Number: 1072954 Registered office: Mortimer House, 37-41 Mortimer Street, London W1T 3JH, UK



## International Journal of Polymeric Materials

Publication details, including instructions for authors and subscription information:

<http://www.informaworld.com/smpp/title~content=t713647664>

## The Effect of Particles Shape on Tensile Properties of Glassy Thermoplastic Composites

L. Nicolais<sup>a</sup>; L. Nicodemo<sup>a</sup>

<sup>a</sup> Istituto di Principi di Ingegneria Chimica, Università di Napoli, Naples, Italy

**To cite this Article** Nicolais, L. and Nicodemo, L.(1974) 'The Effect of Particles Shape on Tensile Properties of Glassy Thermoplastic Composites', *International Journal of Polymeric Materials*, 3: 3, 229 – 243

**To link to this Article:** DOI: 10.1080/00914037408072354

**URL:** <http://dx.doi.org/10.1080/00914037408072354>

PLEASE SCROLL DOWN FOR ARTICLE

Full terms and conditions of use: <http://www.informaworld.com/terms-and-conditions-of-access.pdf>

This article may be used for research, teaching and private study purposes. Any substantial or systematic reproduction, re-distribution, re-selling, loan or sub-licensing, systematic supply or distribution in any form to anyone is expressly forbidden.

The publisher does not give any warranty express or implied or make any representation that the contents will be complete or accurate or up to date. The accuracy of any instructions, formulae and drug doses should be independently verified with primary sources. The publisher shall not be liable for any loss, actions, claims, proceedings, demand or costs or damages whatsoever or howsoever caused arising directly or indirectly in connection with or arising out of the use of this material.

# The Effect of Particles Shape on Tensile Properties of Glassy Thermoplastic Composites

L. NICOLAIS and L. NICODEMO

*Istituto di Principi di Ingegneria Chimica, Università di Napoli, Naples, Italy*

*(Received January 21, 1974)*

Stress-strain curves of composites of styrene-acrylonitrile (SAN) and various fillers such as glass beads, carbospheres,  $\text{CaCO}_3$ , asbestos and glass fibers are reported. The influence of the filler shape and the surface treatment on the Young's moduli, ultimate elongation and strength is analysed on the light of the current knowledge of the crazing phenomena. Existing correlations are checked and extended to the fiber composites.

## INTRODUCTION

Composites are by definition heterogeneous solids consisting of at least two phases of distinct materials. However, the specification of the two materials components in terms of their physical properties and volumetric concentration is insufficient to define the resultant properties of the composite solid. The geometric relationship of the phases with respect to each other defined as the internal material geometry, is often a dominant variable.

In recent years a reasonable amount of work<sup>1-20</sup> has been done on the mechanical behavior of materials reinforced with discontinuous fibers or particulate fillers especially for metals and thermosetting matrices.

The interest in discontinuous fiber composites has been stimulated mainly by the fact that some of the strongest fibers are available only in discontinuous form and discontinuous fibers are more adaptable to certain molding techniques and fabrication of complex shapes than continuous filaments. The interest in particulate composite is due mainly to stiffen the matrix and modify the rheological properties saving the isotropic behavior of the resulting material. However very little experimental work<sup>21-23</sup> has been done using a thermoplastic matrix, in spite of the increasing interest in such materials.

It is the purpose of this study to investigate the effect of the shape of the filler on the tensile properties of thermoplastic composites.

## EXPERIMENTAL

The composites studied were prepared with matrices of styrene-acrylonitrile copolymer<sup>24</sup> (SAN) (Lustran A, Monsanto Co.), and various fillers. The fillers used were:

1) glass beads (Cataphote Corp. type 2740), diameter range 10–44  $\mu$  and density of 2.5 gr/cm<sup>3</sup>, cleaned by refluxing with isopropyl alcohol for 24 h after removing the iron particles present with a large magnet;

2) Carbospheres (General Technologies Corp.) number average particle size: 40  $\mu$  (range 5–160  $\mu$ ) and density of 0.23 gr/cm<sup>3</sup>;

3) Calcium Carbonate cleaned by refluxing with isopropyl alcohol for 24 h;

4) Chopped E-glass fibers supplied by J. Marsville, density 2.5 gr/cm<sup>3</sup> cleaned by refluxing with isopropyl alcohol for 24 h;

5) Crocidolite Asbestos (Asbestos Corp. of America), density 2.5 gr/cm<sup>3</sup>. This material, as received, contained considerable amounts of particulate matter and very short fibers. Much of this was removed by wet screening. Also this filler was cleaned by refluxing with isopropyl alcohol for 24 h.

The composites of styrene-acrylonitrile with glass beads, carbospheres and calcium carbonate were prepared by milling and compression molding. The crude sheets from the two roll mill were cut and then molded in a 3"  $\times$  8" compression mold at 185°C under a pressure of 800 psi for 10 minutes. Specimens containing the following concentrations by volume of filler were prepared: 11, 21, 25 and 43% of glass beads, 12% of Carbospheres, 9, 18 and 25% of calcium carbonate. In the present paper, filler content is always expressed as volume concentration assuming that the density of the matrix is 1.05 and the density of fillers is that previous indicated. Tensile specimens of these composites were cut to the shape specified by ASTM D 686-64 with a high-speed router.

To prepare the short fiber composites the matrix was first compounded with the chopped E-glass or the asbestos fibers to form granular molding compounds of the desired fiber loading.<sup>25</sup> This is essentially a prepregging operation which facilitates handling and reduces fiber damage during subsequent processing steps. The grains were molded in a 3"  $\times$  8" compression mold at 185°C under a pressure of 800 psi for 10 minutes. This process was devised to produce samples with very low void content and thoroughly wetted interfaces.

Specimens containing the following concentrations by volume of filler were

prepared: 16% of fiber glass 0.1 mm long; 16% of fiber glass 0.4 mm long; 8, 14 and 20% of crocidolite asbestos.

The tensile specimens were  $\frac{1}{2}$ " wide strips, 6" long, with a 3" gage length. Tabs were positioned at the ends of the samples to help dissipate clamping stresses.

All samples were annealed at  $T = 90^\circ\text{C}$ , i.e. roughly  $10^\circ\text{C}$  below  $T_g$ , for one day, to minimize molding stresses and then conditioned at  $24^\circ\text{C}$  and  $45 \pm 55\%$  relative humidity for 14 days before testing. The tensile tests were performed at room temperature ( $24^\circ\text{C}$ ) with an Instron Universal testing machine. A constant strain rate of  $0.13 \text{ min}^{-1}$  was used for all samples and strains were monitored with a 1" strain gage length extensometer. Fracture surfaces were examined with a Cambridge electron scanning microscope. All the data reported are the average of at least five specimens.

## RESULTS AND DISCUSSION

In Figures 1 and 2 the stress-strain curves for all the composites analysed are reported and the relative tensile properties are summarized in Table I. The

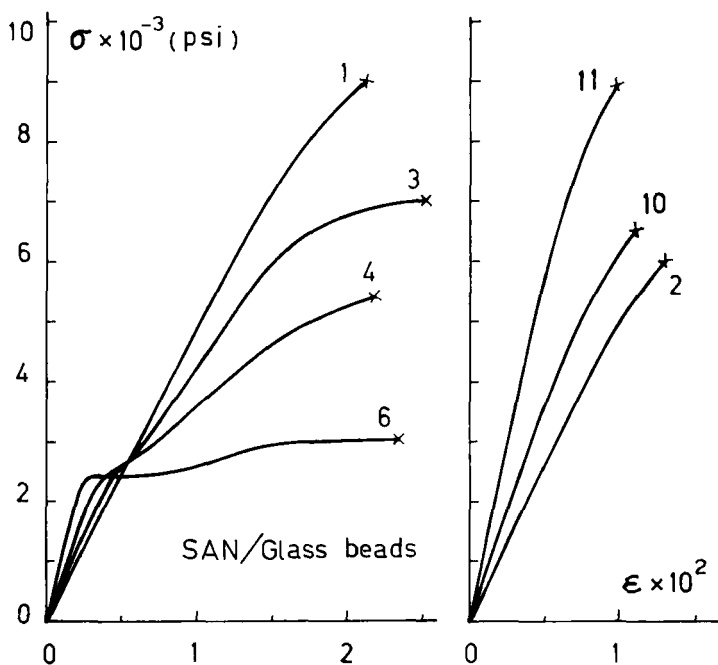


FIGURE 1 Typical stress-strain curves of SAN composites. Designation of samples is given in Table I.

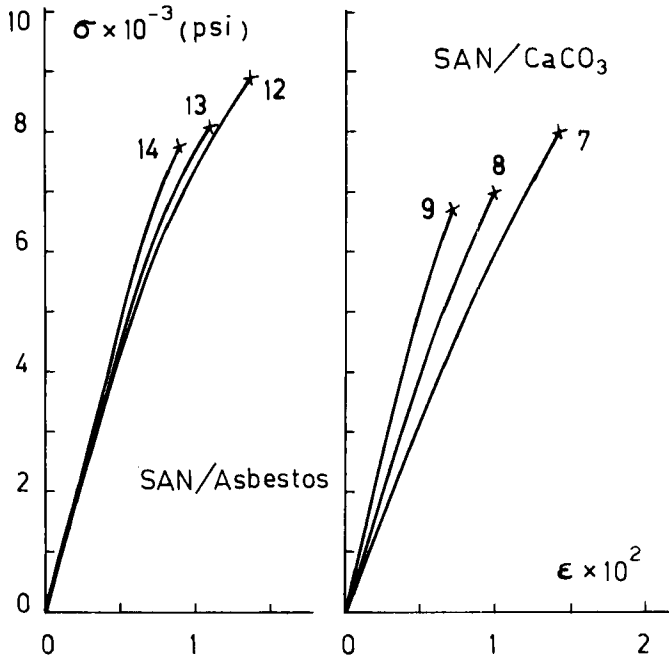


FIGURE 2 Typical stress-strain curves of SAN composites. Designation of samples is given in Table I.

TABLE I  
Properties of the materials studied

Material	$\rho_t$ (gr/cm <sup>3</sup> )	Symbol used	Number of sample	$\emptyset$	$E \times 10^{-5}$ (psi)	$\sigma_u \times 10^{-3}$ (psi)	$\epsilon_u \times 10^2$
SAN	—	▼	1	0	4.4	9.0	2.2
SAN/C	0.23	◇	2	0.12	5.4	6.0	1.3
SAN/glass beads	2.5	▲	3	0.11	5.6	6.9	2.5
			4	0.21	6.8	5.4	2.3
			5	0.25	7.7	4.8	2.4
			6	0.43	11	3.3	2.3
SAN/CaCO <sub>3</sub>	2.5	■	7	0.09	6.2	8.0	1.4
			8	0.18	8.2	6.9	1.0
			9	0.25	10	6.4	0.8
SAN/fiber glass 0.1	2.5	○	10	0.16	7.2	6.5	1.1
SAN/fiber glass 0.4	2.5	△	11	0.16	11.3	8.9	1.0
			12	0.08	8.0	8.8	1.4
SAN/asbestos	2.5	●	13	0.14	8.8	8.2	1.1
			14	0.20	10	7.7	0.9

appearance of the force–deformation response of the glass bead composites is different from the others. In fact while the curves for unfilled SAN and for the other composites do not reach a well-defined yield indicating brittle failure of the material, the curves relative to the glass bead composites show a yield stress<sup>21</sup> which decreases significantly with increasing bead concentration. The curves for these materials, after the initial linear part, exhibit a sudden change in the slope at a well-defined value of stress independent of filler content.

A typical fracture surface for a 20% glass bead composite is shown in Figure 3. The denuded beads indicate that the adhesion of the polymer to the glass is poor as is expected with the composites obtained with fillers cleaned with isopropyl alcohol.

As previously shown<sup>22,26</sup> the addition of cleaned glass beads to a thermoplastic polymer enhances the ultimate elongation due to an inhomogeneous deformational mechanism resulting from formation and propagation of crazes through the polymer. According to Kambour<sup>27</sup> the crazes normally observed in thermoplastic materials are not cracks, but rather localized regions of highly oriented polymer. Then, the high elongation observed in the glass bead filled SAN can be explained assuming that the growth of crazes can be terminated by the glass beads or vacuoles around them. In fact, if the propagating craze encounters a glass sphere to which the matrix is not strongly adherent, interfacial debonding can effectively blunt the tip of the craze and prevent or, at least slow down, further propagation (Figure 3). The elongation at the break is, then, enhanced by the fact that the crazes, which in the unfilled material may nucleate only at singular defects, in the glass bead composites nucleate in the whole specimen because the filler acts as stress riser allowing to reach the critical stress for craze formation. This situation is reflected by the appearance of a knee in the stress–strain curves at a well-defined value of stress which is practically independent of filler content.

The other curves of Figures 1 and 2 do not show a similar behavior. The slope of these curves, after the linear region, changes continuously until the brittle fracture is reached. In particular the curves 7 to 14 are referred to composites with fillers other than spheres while the curve 2 is relative to SAN/carbosphere composites.

As can be seen from Figure 4 the adhesion in this latter case is good and the filler is brittle. The good adhesion prevents the sudden formation of crazes through the whole specimen which causes the sudden change in the slope of the force–deformation curve as previously shown for the glass bead composites. This different behavior between good and poor adhesion has also been reported in Ref. 18. The filler acts as stress riser in a more effective manner in the case of poor adhesion because the dewetting phenomena produces a situation in which the matrix may be considered as filled with voids. Also the brittleness of

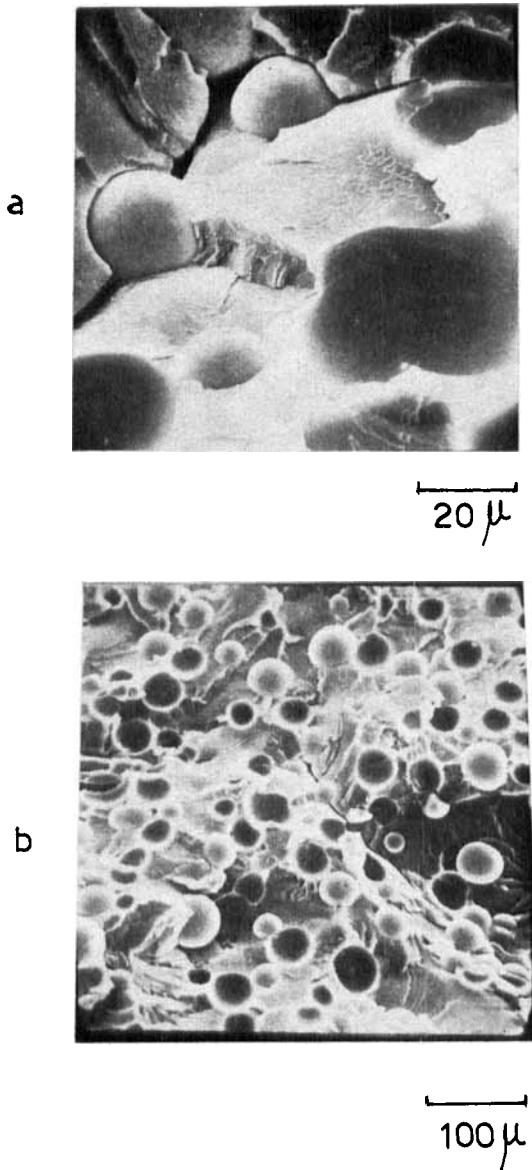


FIGURE 3 Electron scanning photomicrographs of the fracture surface of SAN/glass beads ( $\emptyset = 0.21$ ).

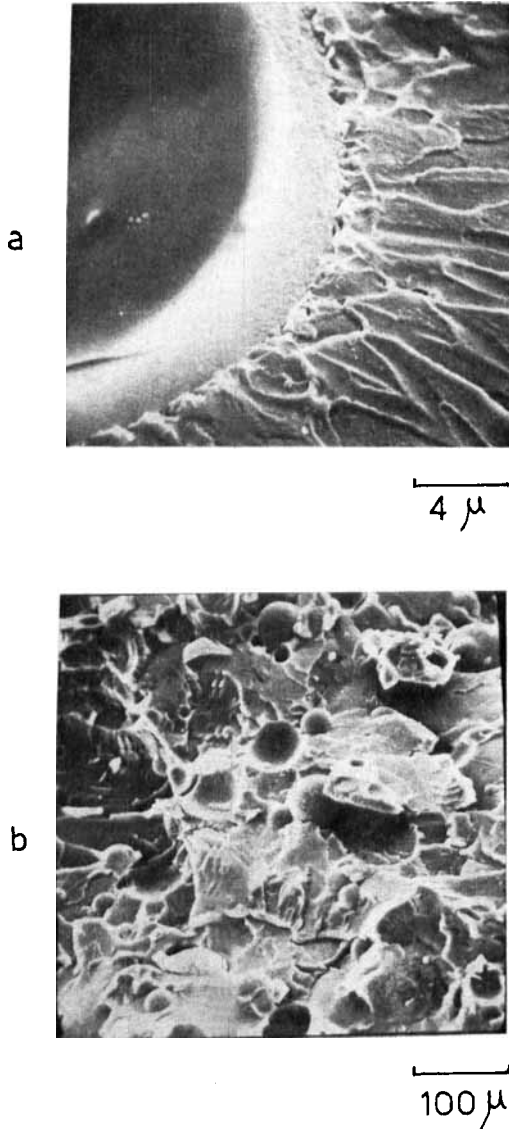


FIGURE 4 Electron scanning photomicrographs of the fracture surface of SAN/carbo-spheres ( $\emptyset = 0.12$ ).



the filler which is in the form of hollow, thin walled spheres of carbon (Figure 4) plays a role on the behaviour of carbosphere composites in the sense that single crazes which nucleate in the matrix are not arrested by the filler but rather break it giving a lower contribution to void formation and consequently to the ultimate elongation with respect to the case of glass bead composites.

This interpretation seems not suitable for the curves 7 to 14 in spite of the similarity of the stress-strain response. These curves are referred to random fiber composites and in particular to asbestos (curves 12-14), fiber glass (curves 10 and 11) and  $\text{CaCO}_3$  (curves 7-9) composites. Also this last material is treated as fiber composite because the shape of the  $\text{CaCO}_3$  is similar to short fibers as can be noticed observing this material with the scanning electron microscope. For all these composites with fibers cleaned with isopropyl alcohol, good adhesion is not achieved as can also be inferred from the observation that the strength of the composites is always lower than that of the unfilled matrix (see Table I). In fact in the case of perfect adhesion, theoretical analysis and experimental results<sup>4,28-31</sup> show that the strength of random short fiber composites is higher than that of the unfilled polymer assuming that the load is distributed between the two components. But, if the fibers are to carry load, the interface must be able to transmit the load through shear stresses to the fibers. In the case of poor adhesion between phases the fibers, of course, cannot sustain much load while the fiber ends act as stress concentrators, reducing the strength of the material.

The poor adhesion existing between glass fibers and SAN can also be seen directly in the micrographs of the fracture surface of such composite shown in Figure 5. An analogous conclusion can be drawn from the micrographs of the fracture surface of SAN/asbestos composite shown in Figure 6. In spite of this poor adhesion, the curves 7 to 14 are similar to curve 2 while the expected behaviour should be similar to that of glass bead composites. This is believed to lie in the random orientation of fibers which causes the craze nucleation to occur gradually due to the different stress concentrations connected with the various orientations of the fibers.

The different behaviour of bead and fiber composites, both with poor adhesion, is reflected by the values of the ultimate elongation  $\epsilon_u$  which are reported vs. the volumetric filler fraction  $\emptyset$  in Figure 7. As can be seen from this figure the values of  $\epsilon_u$  relative to the fiber composites are definitely lower than those of the unfilled polymer while the elongation of the glass bead composites are higher. Moreover, in spite of the poor adhesion, the data relative to fiber composites are fairly well fitted by an equation derived in Ref. 32 assuming perfect adhesion between phases:

$$\epsilon_{u,c} = \epsilon_{u,p}(1 - \emptyset^{1/3}) \quad (1)$$

where the subscripts *c* and *p* are referred to composite and polymer respectively.

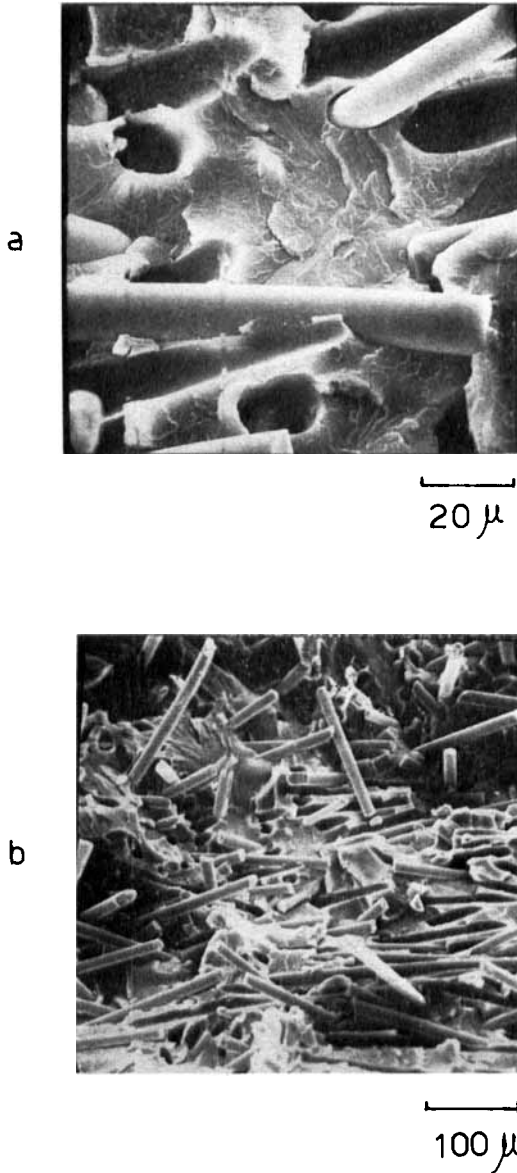


FIGURE 5 Electron scanning photomicrographs of the fracture surface of SAN/glass fibers 0.4 mm long ( $\varnothing = 0.16$ ).

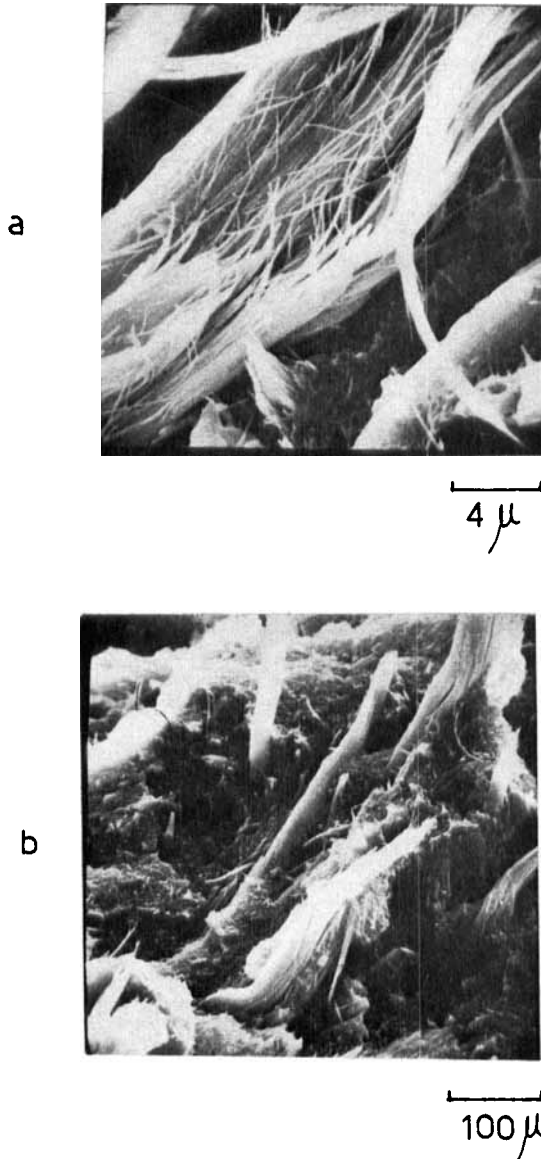


FIGURE 6 Electron scanning photomicrographs of the fracture surface of SAN/asbestos ( $\phi = 0.20$ ).

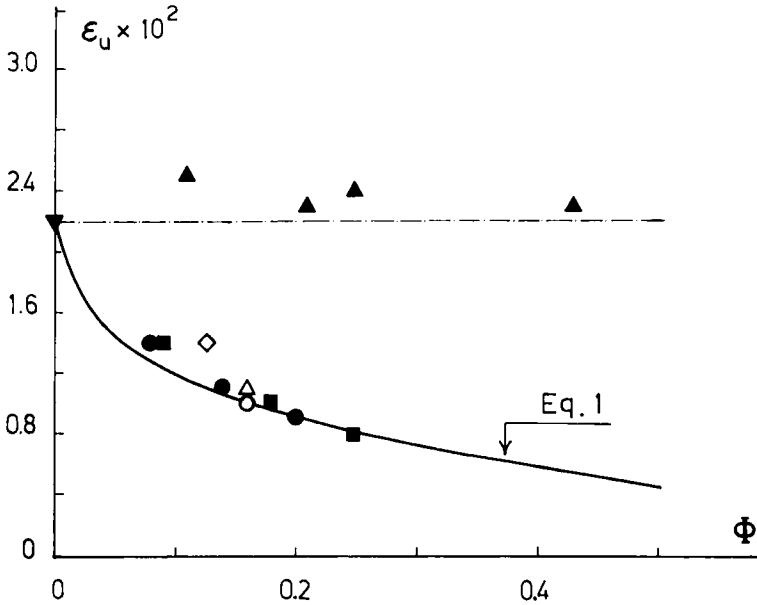


FIGURE 7 Ultimate elongation of composites as a function of filler content. For the symbols refer to Table I.

This can be due to the moderate formation of crazes and vacuoles, as discussed previously, in contrast to the large amount of voids which justifies the high values of  $\epsilon_u$ , even larger than those relative to the unfilled polymer, obtained with the glass bead composites.

However, the poor adhesion present in all the composites studied, except for the SAN/carbospheres, reflects in the reduction of the ultimate strength as shown in Figure 8 where the strength  $\sigma_u$  is reported vs.  $\Phi$ . The data for glass bead composites are well correlated by the equation:

$$\sigma_{u,c} = \sigma_{u,p}(1 - 1.21\Phi^{2/3}) \quad (2)$$

previously proposed.<sup>21</sup>

An extension of this equation has been attempted for the fiber composites rewriting Eq. (2) in the form:

$$\sigma_{u,c} = \sigma_{u,p}(1 - K\Phi^{2/3}) \quad (3)$$

where  $K$  is assumed to be a function of the aspect ratio  $l/d$  being  $l$  and  $d$  the length and the diameter of the fibers respectively. In particular  $K = 1.21$  for spheres. Using Eq. (3) one can correlate the strength data relative to  $\text{CaCO}_3$  and asbestos composites assuming  $K = 0.7$  (curve b) and  $K = 0.35$  (curve c)

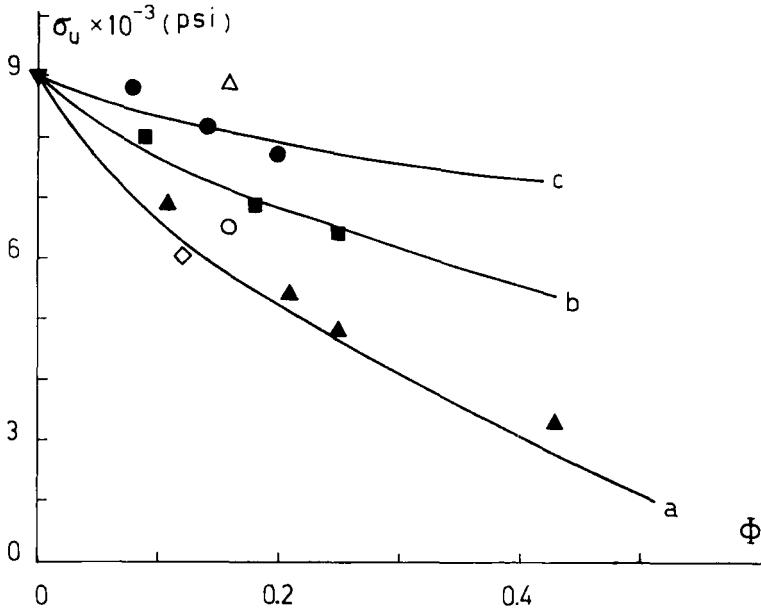


FIGURE 8 Ultimate strength of composites as function of filler content. For the symbols refer to Table I.

respectively. Qualitatively  $K$  seems to decrease with increasing the aspect ratio of the filler as expected by the fact that the increasing aspect ratio reduces the points of stress concentration and enhances the strength fiber efficiency.<sup>28</sup> Analogously the Young's modulus increases with increasing aspect ratio having as a lower bound the modulus of bead composites.

In Figure 9 all the data available of elastic moduli are reported vs. the filler content  $\Phi$ . The curve a represents the well-known Kerner equation:<sup>33</sup>

$$G_c = G_p \left( \frac{1 + AC\Phi}{1 - C\Phi} \right) \quad (4)$$

where

$$A = \frac{7 - 5\mu_p}{8 - 10\mu_p} = 1.17$$

and

$$C = \frac{G_f/G_p - 1}{G_f/G_p + A} = 0.97$$

for this polymer;  $\mu_p$  is the Poisson's ratio of SAN and  $G_f$ ,  $G_p$  and  $G_c$  are the

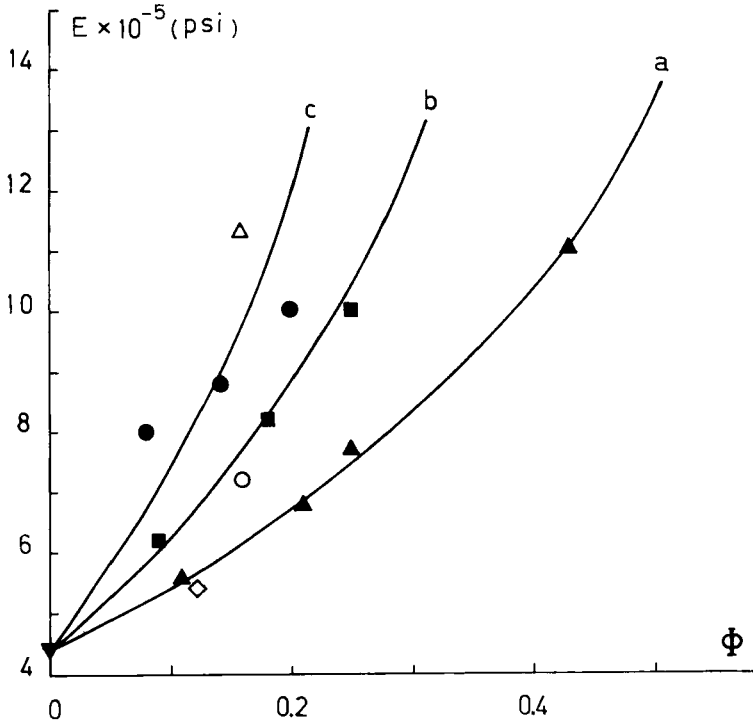


FIGURE 9 Young's moduli of composites as function of filler content. For the symbols refer to Table I.

shear moduli of filler, polymer and composite respectively. Assuming a gross isotropic behavior, i.e.

$$\frac{1 + \mu_p}{1 + \mu_c} \cong 1 \quad (5)$$

where  $\mu_c$  is the Poisson's ratio of the composite, it comes out:

$$\frac{G_c}{G_p} \cong \frac{E_c}{E_p} \quad (6)$$

On the basis of this equation the curve a represents also a correlation for Young's moduli and fits reasonably well the data of glass bead composites. The elastic moduli of fiber composites can be correlated by an equation of the type:

$$\frac{E_c}{E_p} = \exp A\phi \quad (7)$$

where  $A$  assumes the values of 3.5 for the  $\text{CaCO}_3$  composites (curve b) and the

value of 5 for the asbestos composites (curve c) showing that also this parameter  $A$  seems to increase with aspect ratio of the filler.

In conclusion it has been shown that the main difference between the tensile behavior of fiber and bead composites, both with poor adhesion, lies in the ultimate elongation which in the case of the former decreases with volume fraction according to an equation derived for perfect adhesion while the ultimate elongation of glass bead composites is even higher than that of unfilled polymer. The strength and the modulus are increased with aspect ratio analogously to the case of perfect adhesion. The strength of composites, however, remains always lower than that of the unfilled polymer due to the poor adhesion between phases while the modulus is always higher.

## References

1. A. Kelly and W. R. Tyson, *J. Mech. Phys. Solids* **13**, 329 (1965).
2. H. I. Cox, *Brit. J. Appl. Phys.* **3**, 72 (1952).
3. J. K. Lees, *Polym. Eng. Sci.* **8**, 186 (1968).
4. J. K. Lees, *Polym. Eng. Sci.* **8**, 195 (1968).
5. S. W. Tsai and P. E. Chen, Monsanto/Washington University ONR/ARPA Association Second Annual Project Review and Technical Report HPC 67-28, AD 658 533, p. 13 (1967).
6. R. M. Anderson and R. E. Lavengood, *SPE J.* **24**, 20 (1968).
7. O. Ishai and R. E. Lavengood, Monsanto/Washington University ONR/ARPA Association Report HPC 68-74 (1969).
8. C. Zweben, Tensile Strength of Fiber-Reinforced Composites: Basic Concepts and Recent Developments, presented at the ASTM Conference on Composite Materials: Testing and Design, New Orleans, La., Feb. 1969.
9. W. R. Tyson and G. J. Davis, *Brit. J. Appl. Phys.* **16**, 199 (1965).
10. D. M. Schuster and E. Scala, *AIAA J.* **6**, 527 (1968).
11. L. J. Cohen and J. P. Romualdi, *J. Franklin Inst.* **284**, 388 (1967).
12. J. L. Kane, *J. Composite Materials* **1**, 2 (1967).
13. A. Kelly, *Strong Solids*, Oxford University Press (1966).
14. G. S. Holister and C. Thomas, *Fiber Reinforced Materials*, Elsevier Publishing Co. (1966).
15. N. F. Dow, Study of Stresses Near a Discontinuity in a Filament-Reinforced Composite Metal, General Electric Co. Report TIS R63SD61, Aug. 1963.
16. W. H. Sutton and J. Chorné, Potential of Oxide-Fiber Reinforced Metals, Fiber Composite Materials, American Society for Metals (1965).
17. M. J. Owen, T. R. Smith and R. Dukes, *Plastics and Polymers*, June 1969.
18. S. Sahu and L. J. Broutman, *Polymer Eng. Sci.* **12**, 91 (1972).
19. A. S. Kenyon and H. J. Duffy, *Polymer Eng. Sci.* **7**, 1 (1967).
20. L. Nicolais and L. Nicodemo, *Polymer Eng. Sci.* **13**, 469 (1973).
21. L. Nicolais and M. Narkis, *Polymer Eng. Sci.* **11**, 194 (1971).
22. R. E. Lavengood, L. Nicolais and M. Narkis, *J. Appl. Polymer Sci.* **17**, 1177 (1973).
23. L. A. Goettler, Flow Orientation of Short Fibers in Transfer Molding, 25th Annual Technical Conference, 1970—Reinforced Plastic/Composites Division, The Society of the Plastics Industry, Inc. Section 14-A, p. 1.
24. J. R. Joseph, J. L. Kardos and L. E. Nielsen, *J. Appl. Polymer Sci.* **12**, 1151 (1968).
25. R. M. Anderson and D. C. Morris, Encapsulated Short Fiber Molding Compounds, Proceedings of 23rd Annual Technical Conference, Society of Plastics Industry (1968) p. 17E.
26. L. Nicolais, E. Drioli and R. F. Landel, *Polymer*, **14**, 21 (1973).

27. R. P. Kambour, *Appl. Polymer Symp.* **N7**, 215 (1968).
28. P. E. Chen, *Polymer Eng. Sci.* **11**, 51 (1971).
29. M. Horio and S. Onogi, *J. Appl. Physics* **22**, 971 (1951).
30. J. E. Ashton, J. C. Halpin and P. H. Petit, *Primer on Composite Materials: Analysis*, Technomic, Stamford, Conn. 1969.
31. W. B. Rosen (Ed.), *Fracture Processes in Polymeric Solids*, Wiley (1967).
32. L. E. Nielsen, *J. Comp. Materials* **1**, 100 (1967).
33. E. H. Kerner, *Proc. Phys. Soc.* **69B**, 808 (1956).